Report on the outcomes of a Short-Term Scientific Mission[1]

Action number: CA21119

Grantee name: Claudia Frangipani

Details of the STSM

Title: Application of cloud cover algorithms based on broadband radiation measurements to cloud screening in AOD photometry.

Start and end date: 10/03/2024 to 10/04/2024

Description of the work carried out during the STSM

Description of the activities carried out during the STSM. Any deviations from the initial working plan shall also be described in this section.

The study focused on data from July 2023, when measurements and products from different instruments are simultaneously available. Broadband radiation data, both shortwave (global, diffuse and direct normal components – respectively SWD, DIF and DNI) and downward longwave, are collected within the Baseline Surface Radiation Network framework. Spectral sun irradiance for AOD retrieval is measured by different instruments: CIMEL, whose data are processed by both AERONET and CAELIS (GOA, University of Valladolid) algorithms, and PFR. The OMEA all-sky camera data are yielded by three different algorithms developed by GOA (University of Valladolid): one that predicts cloud fraction (CF), one that determines whether the sun is clear (unobstructed) or not, one that computes CF from the image taken; only the last two were used in this study.

Broadband radiation measurements were processed with two different codes: RADFLUX and BrightSun, instead of implementing Long et al. and APCADA, as stated in the application form. It was decided to apply RADFLUX because it includes both Long et al. and APCADA algorithms, the latter in a revised version, and it yields different information, among which: a clear-sky flag, the clear sky equivalent SW and LW values and CF, using both shortwave (SWD and DIF) and longwave broadband radiation data. BrightSun was chosen because it allows to implement both clear-sky and clear-sun models, flagging data accordingly, and thus is more appropriate for the analysis of AOD retrieval cloud screening process. Clear-sky models: BrightSunCSDc, Inman and Ellis were selected as clear-sky models; BrightSunCSDs, Gueymard, Larraneta, RuizArias, and Zhao as clear-sun models.

[1] This report is submitted by the grantee to the Action MC for approval and for claiming payment of the awarded grant. The Grant Awarding Coordinator coordinates the evaluation of this report on behalf of the Action MC and instructs the GH for payment of the Grant.

To start, RADFLUX and BrightSun were implemented so to obtain clear-sky flags and clear-sun flags, in addition to SW and LW CF, for comparison with all-sky camera data.

Then, the issue of photometer time homogenization was addressed. CIMEL measurements (both AERONET and CAELIS) are not made (or at least, saved) at HH:MM:00, unlike PFR, broadband radiometer and all-sky camera data. Therefore, AERONET and CAELIS data within 30 seconds of each other were deemed simultaneous and rounded to the closest minute. Despite the timestamp manipulation to homogenize the data set, comparison of CIMEL data to others is difficult: too few data match. There are especially very few common measurements with the all-sky camera, whose resolution is 5 minutes, for SZA smaller than 80°. Therefore, the inter-comparison of cloud screening results from the different methods relies on PFR data.

The last part of the work consisted in evaluating how well PFR, all-sky camera and models clear/cloud flagged data match, how often mismatches occur and what influences them. Particular attention was dedicated to data deemed clear by the PFR but cloudy by the all-sky camera algorithm.

Description of the STSM main achievements and planned follow-up activities

Description and assessment of whether the STSM achieved its planned goals and expected outcomes, including specific contribution to Action objective and deliverables, or publications resulting from the STSM. Agreed plans for future follow-up collaborations shall also be described in this section.

The intercomparison of the different methods highlights various issues.

First, the time resolution and "time shift" between measurements make difficult the comparison between cloud screening process results, either because of the number of common observations or because of the possible rapid change of sky conditions between measurements taken at slightly different times, crucial for the determination of whether the sun is obstructed or not. Products from all-sky camera are to be considered instantaneous but have a 5-minutes resolution for solar zenith angles less than 80°. Results from broadband measurements, whether obtained with RADFLUX or BrightSun, depend on the input data resolution, in this case, 1 minute. PFR measures every minute, with only an exposure of a few seconds, CIMEL instead makes measurements in triplets. As stated above, it was chosen to focus on PFR data as, e.g., CIMEL-AERONET has only 479 observations in common with the all-sky camera.

Second, photometer cloud screening criteria are necessarily strict and successfully delete most of the cloudy data. Matches between clear and cloud flags for PFR, all-sky camera and clear-sun models are summarized in Table 1. The lowest matching percentage is found for PFR-all sky camera, although there is perfect agreement for over 50% of the common measurements. Three different PFR clear flag – camera cloud flag mismatch cases are discussed, and three figures are shown for each. The first shows an overview (and a zoomed view) of, in descending order:

- broadband measurements,
- clear sky flags for clear-sky models,
- clear flagged observations by photometers,
- unobstructed/obstructed sun flag for all-sky camera,
- cloud flagged observations by photometers,
- clear sun flags for clear-sun models (if missing, detected as cloudy),
- cloud fraction by RADFLUX and all-sky camera algorithm.

(A detailed explanation of the legend can be found in Table 2, last page). The second image shows AOD (500 nm) vs Ångström α coefficient for flagged values (orange PFR clear flag – camera cloud flag mismatch) and the third shows images from another sky camera to verify the cloud screening process.

Normally, PFR clear/cloud detection is more reliable: an example is 16 July 2023. 6:15 and 6:20 UTC measurements are detected as clear, confirmed by the AOD and α values (Figure 2), but all-sky camera and clear-sun models detect them as cloudy (Figure 1 and Figure 3).

Some mismatch cases are instead hard to judge, like for 13 July 2023 between 17:20 and 17:45 UTC. PFR detects the sun as unobstructed, whereas the all-sky camera and clear-sun models as cloudy (with the exception of BrightSunCSDs for 17:40 UTC), see Figure 4. Looking at the all-sky camera images (Figure 6) is difficult to determine whether there are clouds in front on the sun or not although it would appear so, but values of AOD and α (Figure 5) would suggest there are none.

Yet, a few cases when PFR fails cloud detection occur, especially for cirrus clouds, e.g. 22 July 2023 14:50 UTC. The all-sky camera, broadband radiation measurements and both BrightSun and RuizArias models detect a cirrus cloud in front of the sun as it can be seen in Figure 7 and Figure 9 (central image), but the PFR cloud screening algorithm fails to detect it. Although, it is true that such isolated case would be deemed an outlier in further analysis (Figure 8).

Last, no relationship between PFR clear/cloud flags and cloud fraction, either estimated by RADFLUX or all-sky camera algorithm can be extrapolated, except for when CF is 0 or 1 (totally cloud free sky or totally overcast sky). CF can be any value in between 0 and 1 and the sun can be unobstructed, or a cloud could be in front of the sun even if the sky is mostly cloud-free, as shown in Figure 10 where CF was divided in 10 bins and for each is given the number of clear and cloudy flags.

In the framework of the HARMONIA objectives, the analysis carried out in this project and results obtained are consistent with WG1 Task T.1 and Deliverable D1.2 “Report on the differences and uncertainties related to standard products provided from already existing analysis algorithms”, and WG2 task T2.2: “Analysis of the collected measurements and presentation of the results on measurement improvements”, as it supports AOD retrieval activities, evaluating Cloud Screening methods and the instrumental synergetic approach that HARMONIA wants to promote (WG1, WG2, WG4). Moreover, this study involved three groups involved in HARMONIA from three different countries: CNR-ISP (Bologna, IT), DWD MOL-RAO (Lindenberg, DE) and University of Valladolid GOA (Valladolid, ES).

Possible future developments are: analysis of an extended data set, including PREDE instruments, focusing on mismatches between instruments, models and all-sky camera occurring at very low or very high values of Ångström α coefficient; analysis with a higher temporal resolution for all-sky camera products (especially cloud flagging) going to every minute or lower; investigation of whether the different sensibility of LW and SW broadband radiation to cirrus clouds can be of any use in case of mismatches between instruments.

Table 1: number of common observations and agreement between clear-sun/cloud flags of PFR, clear-sun models and all-sky camera algorithm.

x	y	common obs	clear – clear or cloudy – cloudy perfect match	clear (x) – cloudy (y) mismatch	cloudy (x) – clear (y) mismatch
PFR	All-sky camera	2722	65%	3%	32%
BrightSun	All-sky camera	4954	88%	1%	11%
RuizArias	All-sky camera	4954	81%	0.1%	18.9%
BrightSun	PFR	15199	77%	17%	6%
RuizArias	PFR	15199	79%	5%	16%

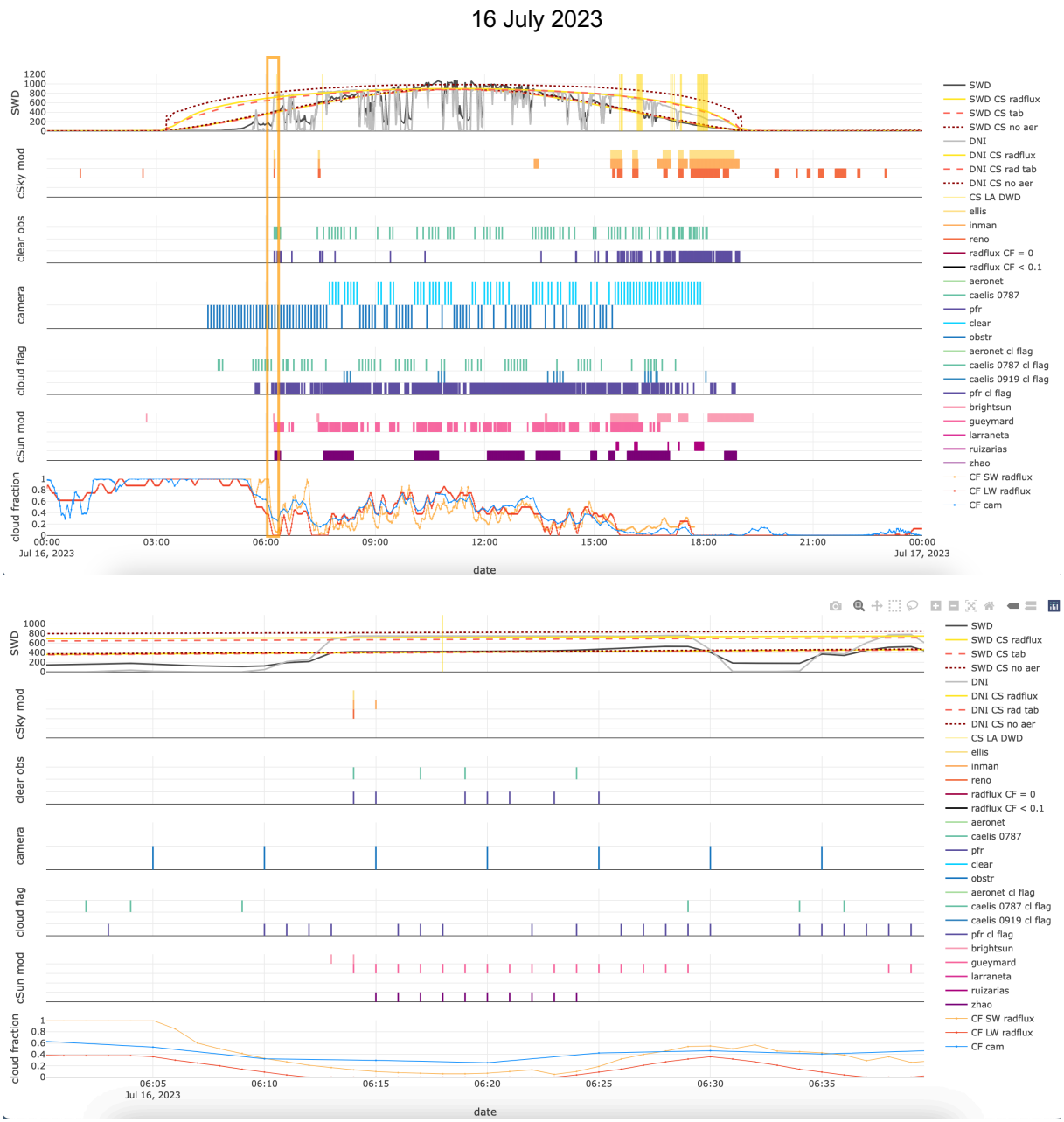

Figure 1: overview of all measurements, products and flags for 16 July 2023. The PFR clear – camera cloud flag mismatches occur at 6:15 and 6:20 UTC, highlighted by the orange. Bottom image shows a zoomed in view. See Table 2 for detailed legend explanation.

Figure 2: AOD vs Ångström α coefficient for PFR, 16 July 2023. Values confirm that the sun is clear: α coefficient is larger than 1.5 and AOD is low. Light and dark green points represent clear and cloud flagged observations, respectively. Orange points indicate PFR clear flag – camera cloud flag mismatch, yellow for the opposite mismatch.

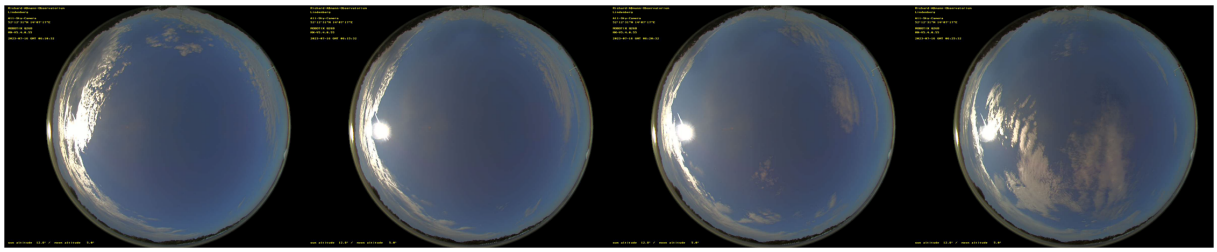

Figure 3: All-sky camera images between 06:10 and 06:25 UTC, 16 July 2023. Sun is clear for 6:15 and 6:20 UTC (second and third picture), although a cloud is very near. PFR correctly identifies these two observations as clear but both all-sky camera algorithm and clear-sun models flag them as cloudy.

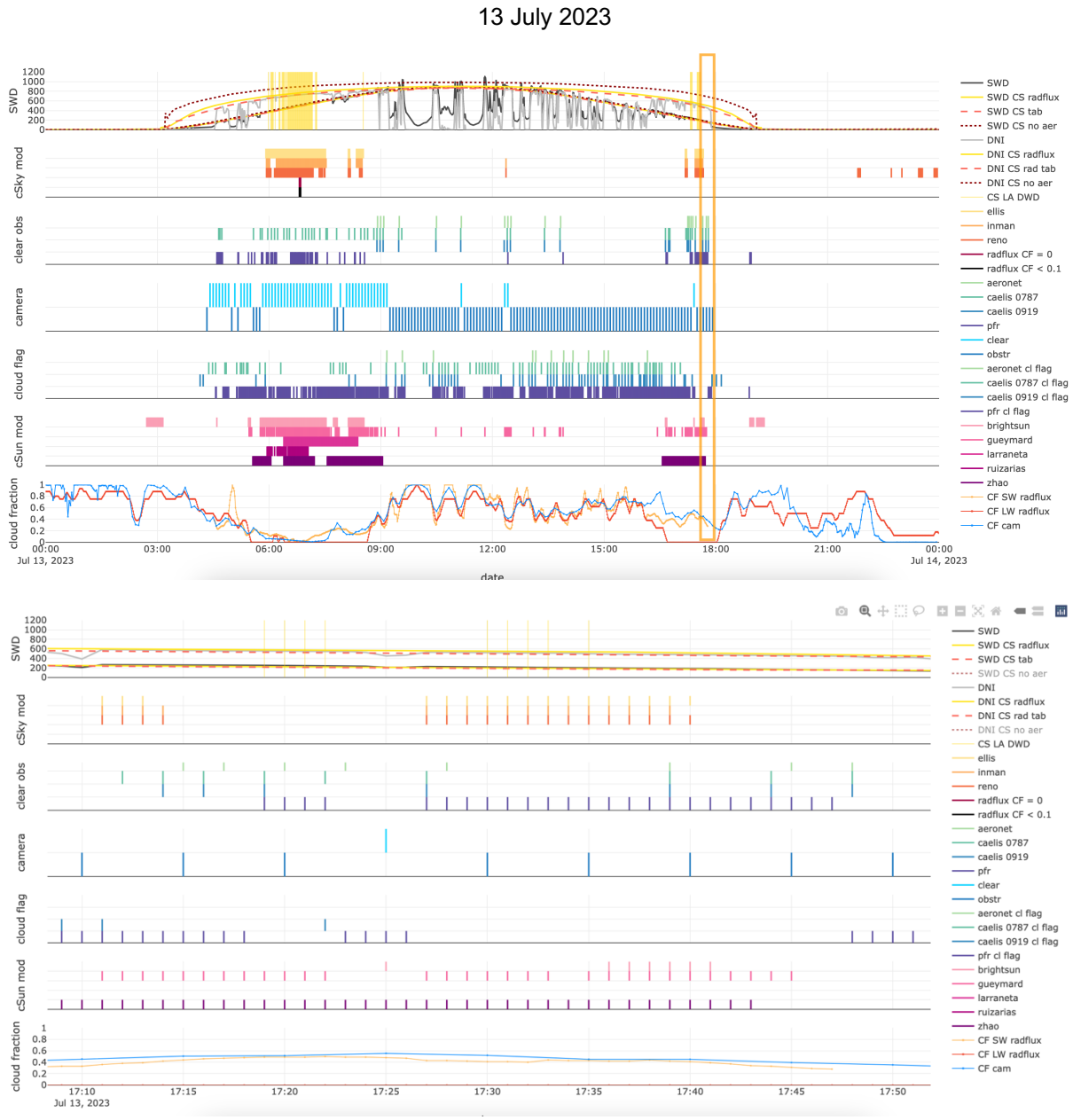

Figure 4: overview of all measurements, products and flags for 13 July 2023. PFR clear – camera cloud flag mismatches occur between 17:20 and 17:40 UTC, highlighted by the orange box. Bottom image shows a zoomed in view. See Table 2 for detailed legend explanation.

Figure 5: AOD vs Ångström α coefficient for PFR, 13 July 2023. AOD and α coefficient values suggest that the sun is clear. Light and dark green points represent clear and cloud flagged observations, respectively. Orange points indicate PFR clear flag – camera cloud flag mismatch, yellow for the opposite mismatch.

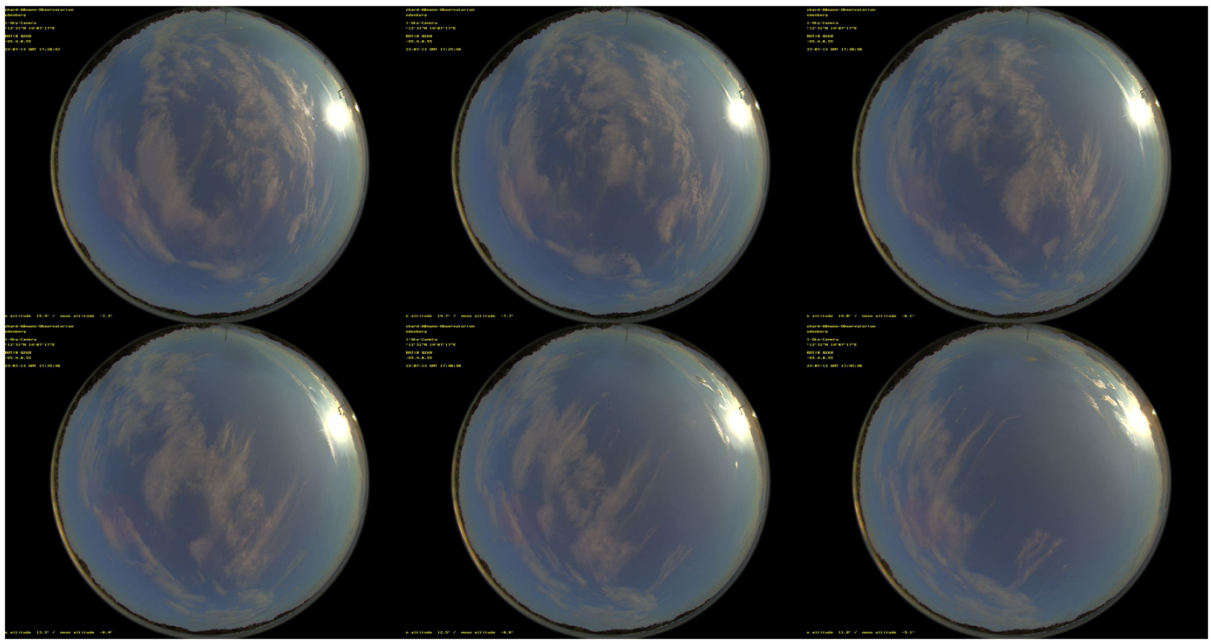

Figure 6: All-sky camera images between 17:20 - 17:45 UTC, 13 July 2023. This is an example of cases when it is difficult to evaluate whether the sun is obstructed or not from a visual evaluation. PFR identifies these six observations as clear, whereas all-sky camera algorithm identifies the sun as obstructed for these six moments. RuizArias model flags them all as cloudy, BrightSun too, with the exception of 17:40 UTC (central image, second row).

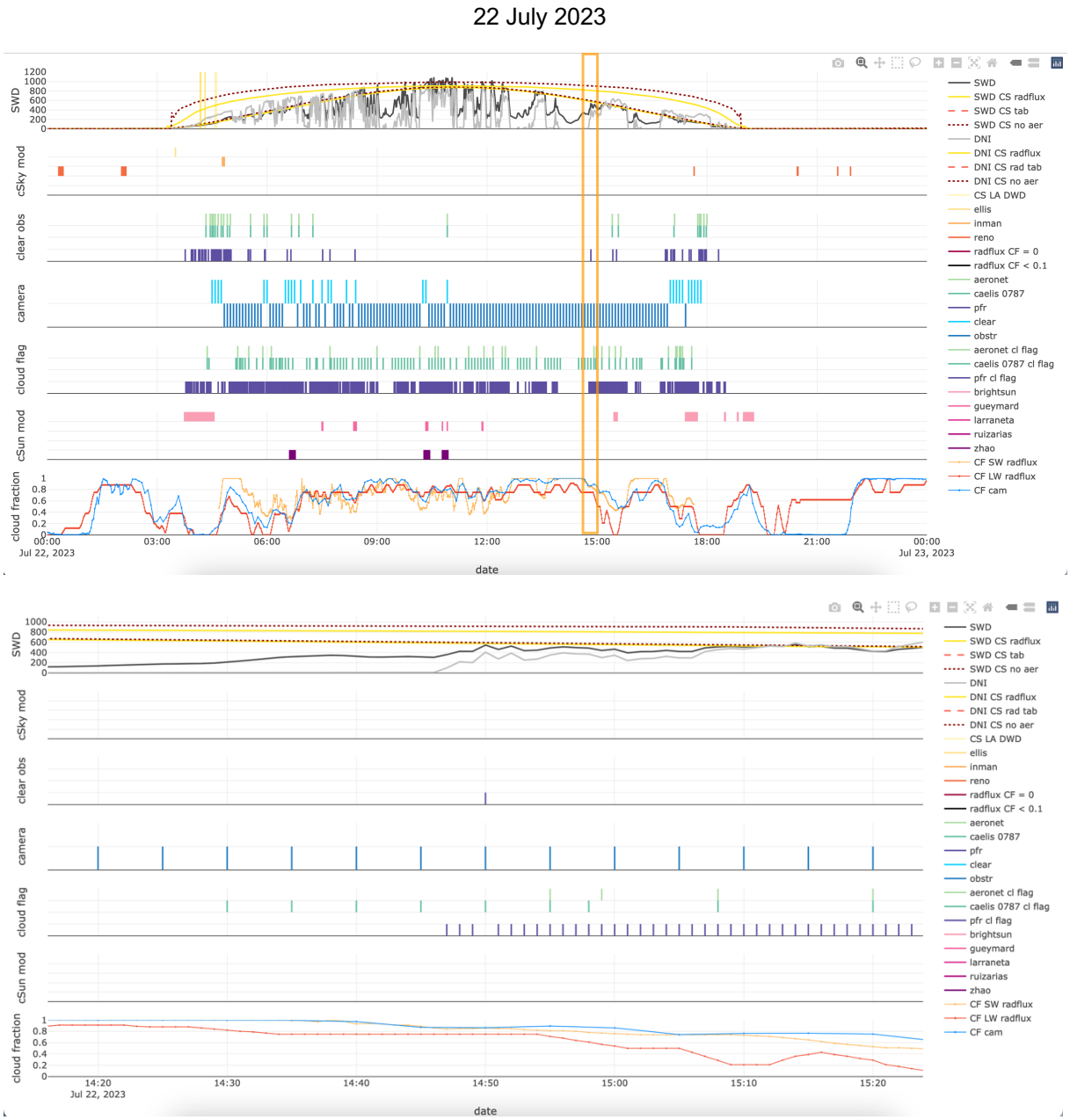

Figure 7: overview of all measurements, products and flags for 22 July 2023. PFR clear – camera cloud flag mismatch occurs at 14:50 UTC, highlighted by the orange. Bottom image shows a zoomed in view. See Table 2 for detailed legend explanation.

Figure 8: AOD vs Ångström α coefficient for PFR, 22 July 2023. Based on AOD and coefficient, 14:50 UTC seems to be an outlier (point on the left, AOD ~ 0.7 and $\alpha \sim 0.5$), although it passed the cloud screening and was identified as clear. Light and dark green points represent clear and cloud flagged observations, respectively. Orange points indicate PFR clear flag – camera cloud flag mismatch, yellow for the opposite mismatch.

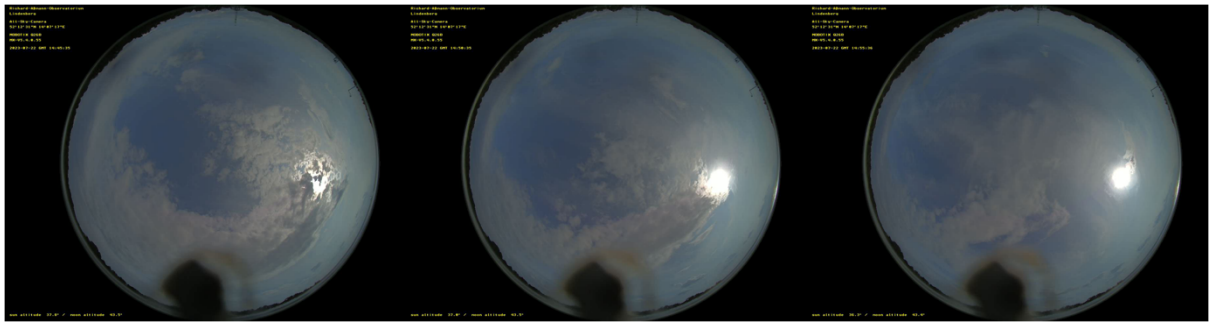

Figure 9: All-sky camera images between 14:45 and 14:55 UTC, 22 July 2023. Sun is clearly obstructed by a cirrus cloud at 14:50 UTC (central image) but PFR identifies the measurement as clear. Both BrightSun and RuizArias models instead correctly flag the observation as cloudy.

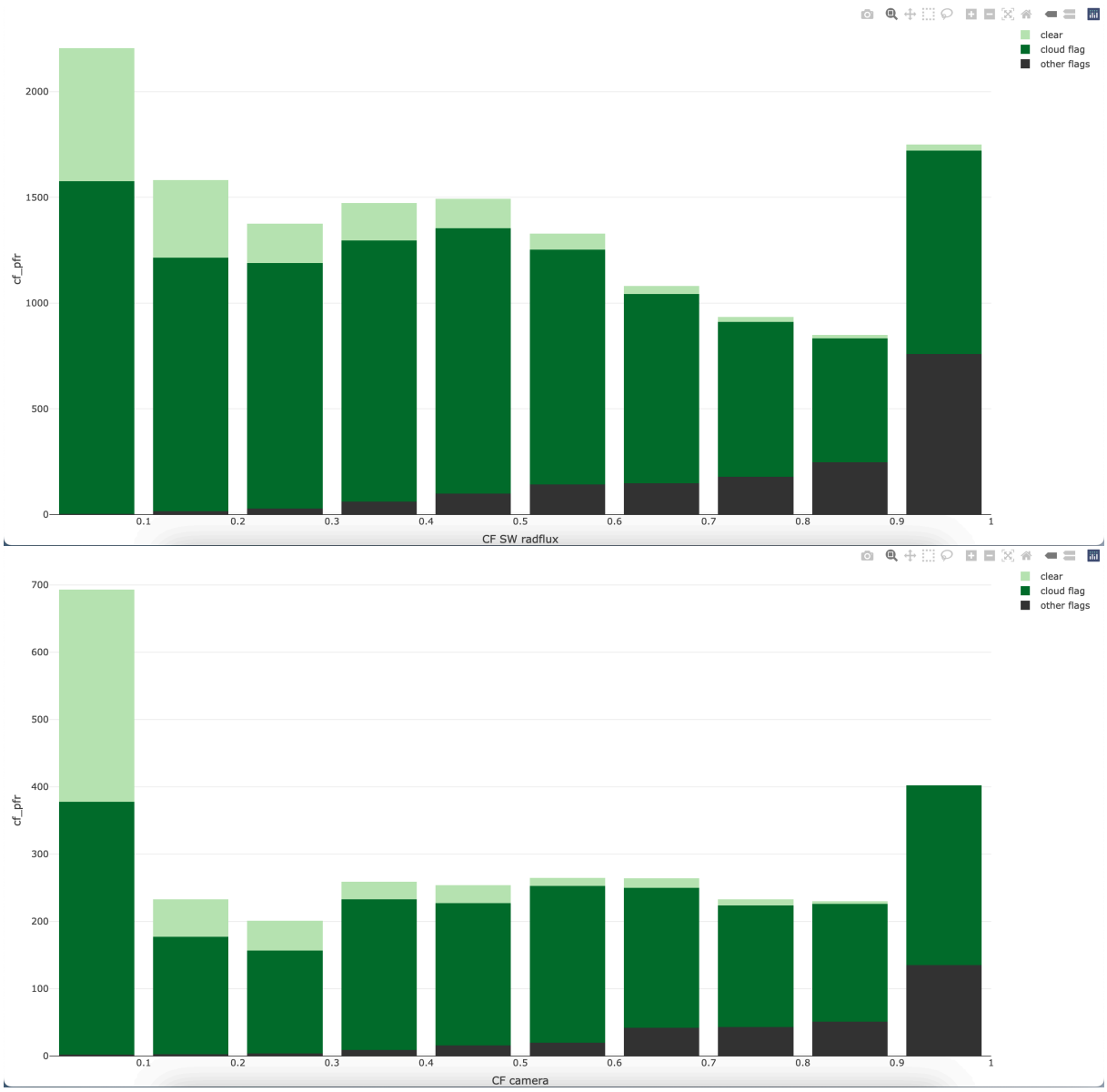

Figure 10: PFR clear and cloud flag count, light and dark green respectively, by cloud fraction divided in 0.1 bins. CF is estimated by RADFLUX (upper image) and all-sky camera algorithm (bottom image). No relationship can be extrapolated, as the sun can be unobstructed or obstructed, regardless of the cloud cover of the rest of the sky, although obviously the more overcast the sky conditions are, the less likely it is for the sun to be cloud-free (CF = 0 and CF = 1 are excluded from the binning).

Table 2: Detailed legend explanation of Figures 1, 4 and 7, from top to bottom graph.

Plot 1	SWD / DNI CS radflux CS tab CS no aer CS LA DWD	Measured global shortwave / direct normal irradiance (W/m^2) clear sky component as computed by RADFLUX clear sky component computed by radiative transfer model clear sky component computed by radiative transfer model without aerosol "in house" clear sky flag computed following Long and Ackerman (2000)
Plot 2	Ellis, Inman, Reno RADFLUX CF = 0 RADFLUX CF = 1	*Clear-sky* flags for the respective clear-sky models available for computation with BrightSun *Missing segments mean cloud flagged observation* observations with shortwave cloud fraction = 0, by RADFLUX observations with shortwave cloud fraction < 0.1, by RADFLUX
Plot 3	Aeronet CAELIS 0787 CAELIS 0919 PFR	CIMEL clear obs flag by AERONET algorithm CIMEL 0787 clear obs flag by CAELIS algorithm CIMEL 0919 clear obs flag by CAELIS algorithm clear obs flag for PFR
Plot 4	clear obstr	clear / unobstructed sun flag by all-sky camera algorithm obstructed sun flag by all-sky camera algorithm
Plot 5	Aeronet cl flag CAELIS 0787 cl flag CAELIS 0919 cl flag PFR cl flag	CIMEL cloud flag by AERONET algorithm CIMEL 0787 cloud flag by CAELIS algorithm CIMEL 0919 cloud flag by CAELIS algorithm cloud flag for PFR
Plot 6	BrightSun, Gueymard, Larraneta, RuizArias, Zhao	*Clear-sun* flags for the respective clear-sun models available for computation with BrightSun *Missing segments mean cloud flagged observation*
Plot 7	CF SW RADFLUX CF LW RADFLUX CF cam	Cloud fraction estimated by RADFLUX, based on shortwave meas Cloud fraction estimated by RADFLUX, based on longwave meas Cloud fraction estimated by all-sky cam algorithm

Bibliography

Bright et al. (2020): *Bright-Sun: A globally applicable 1-min irradiance clear-sky detection model*. doi: 10.1016/j.rser.2020.109706

González et al. (2020): *Daytime and nighttime aerosol optical depth implementation in CÆLIS*. doi: 10.5194/gi-9-417-2020

Long and Ackerman (2000): *Identification of clear skies from broadband pyranometer measurements and calculation of downwelling shortwave cloud effects*. doi: 10.1029/2000JD900077

Riihimaki et al. (2019): *Radiative Flux Analysis (RADFLUXANAL) Value-Added Product: Retrieval of Clear-Sky Broadband Radiative Fluxes and Other Derived Values.* doi: 10.2172/1569477